# Supplementary Materials: Effect of Electronic Conductivities of Iridium Oxide/Doped $SnO_2$ Oxygen-Evolving Catalysts on the Polarization Properties in Proton Exchange Membrane Water Electrolysis

**Hideaki Ohno [1], Shinji Nohara [2,3], Katsuyoshi Kakinuma [3], Makoto Uchida [3], and Hiroyuki Uchida [2,3,*]**

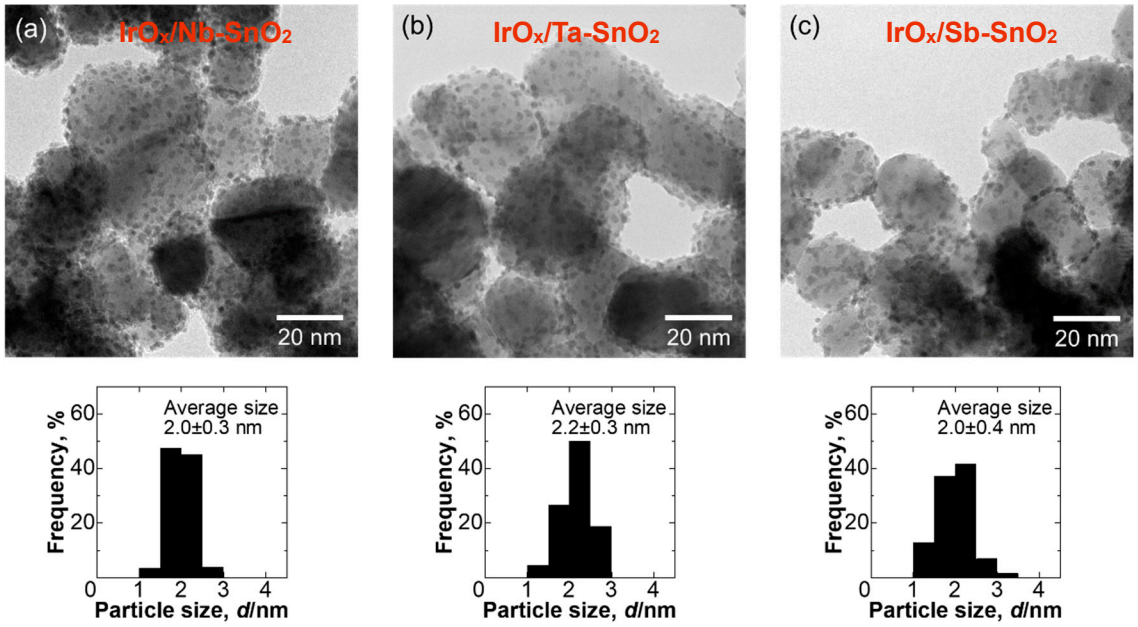


**Figure S1.** TEM images and particle size distribution histograms for (a) $IrO_x$/Nb-$SnO_2$, (b) $IrO_x$/Ta-$SnO_2$, and (c) $IrO_x$/Sb-$SnO_2$ catalysts. Those for (a) $IrO_x$/Nb-$SnO_2$ and (b) $IrO_x$/Ta-$SnO_2$ are cited from our previous work [1] to compare the dispersion states and particle size distributions of $IrO_x$ with (c) $IrO_x$/Sb-$SnO_2$, which is shown in Figure 1 of the text.

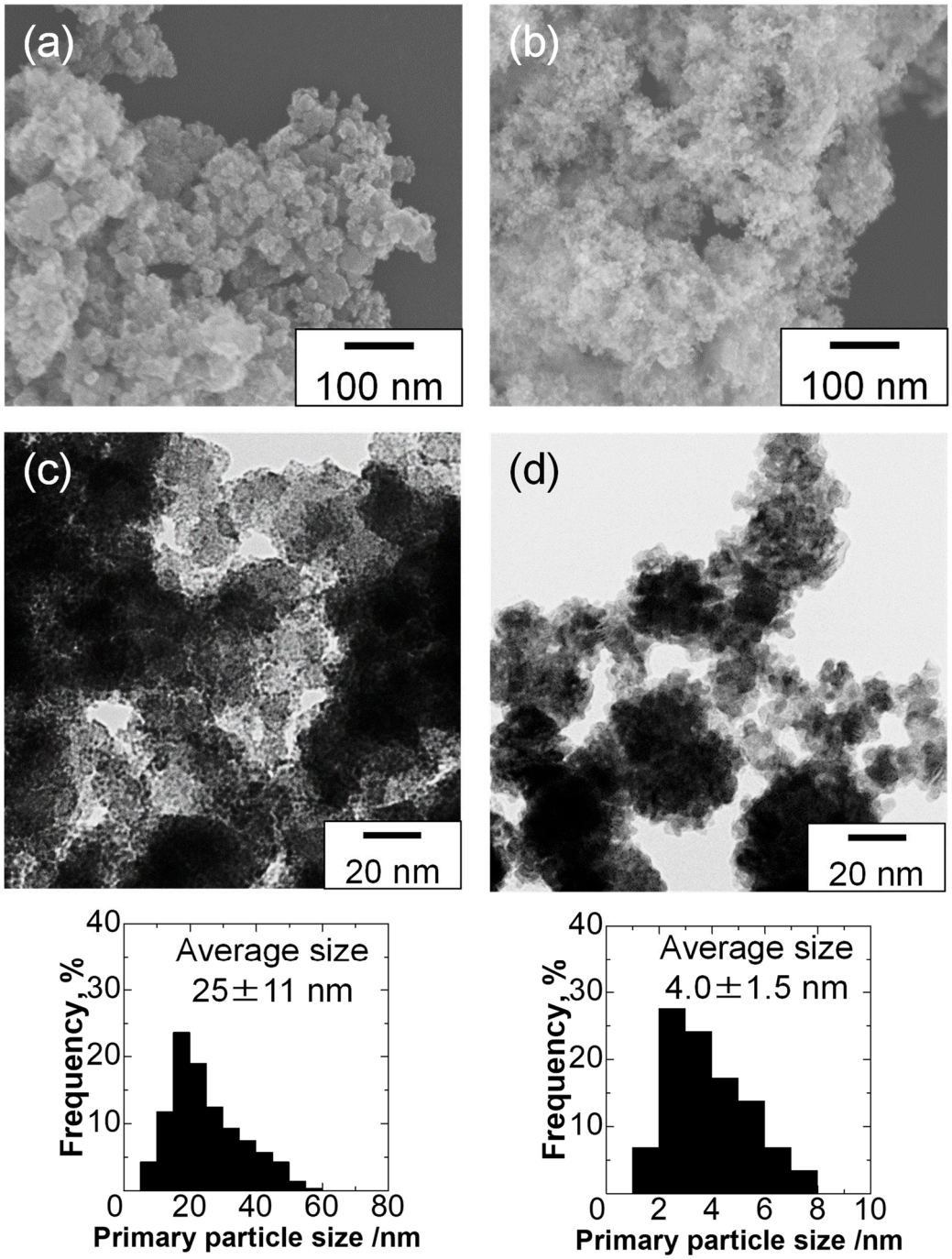


**Figure S2.** Scanning electron microscopic (SEM) and transmission electron microscopic (TEM) images and primary particle size distribution histograms (primary particles) for conventional catalysts: (a,c) commercial $IrO_2$ and (b,d) commercial Pt black.

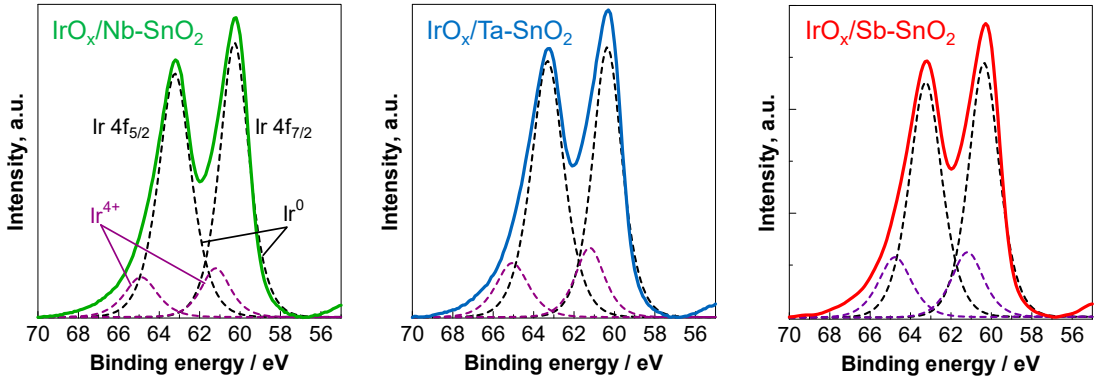


**Figure S3.** X-ray photoelectron spectra (XPS) of $IrO_x$/M-$SnO_2$ (M = Nb, Ta, and Sb) catalysts. Those for $IrO_x$/Nb-$SnO_2$ and $IrO_x$/Ta-$SnO_2$ are cited from our previous work [1] to compare the electronic states of $IrO_x$. Peaks around 64 and 60 eV were assigned to Ir $4f_{5/2}$ and $4f_{7/2}$, respectively. These peaks were deconvoluted into symmetric Gaussian peaks corresponding to $Ir^0$ (metallic Ir) and $Ir^{4+}$ ($IrO_2$) components.

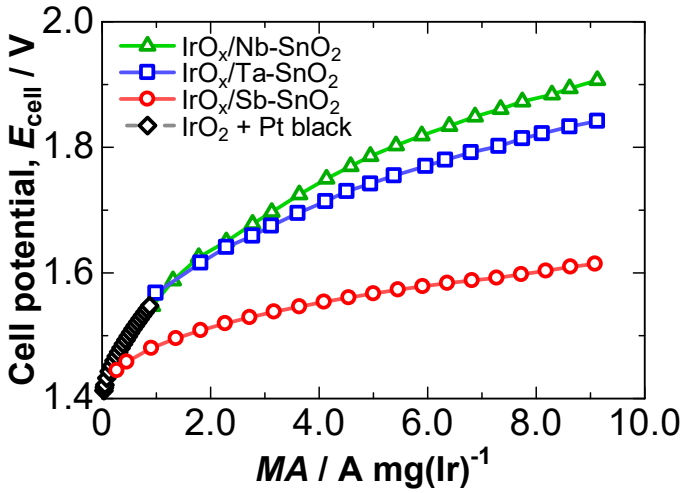


**Figure S4.** Steady-state *I-E* curves of single cells with various anodes and Pt/GCB cathode at 80 °C. The current is shown as the apparent mass activity (*MA*) based on the mass of Ir loaded in the anode catalyst layers. Ultrapure water was supplied to the anode with a flow rate of 40 mL $min^{-1}$. The cathode compartment was purged with $H_2$.

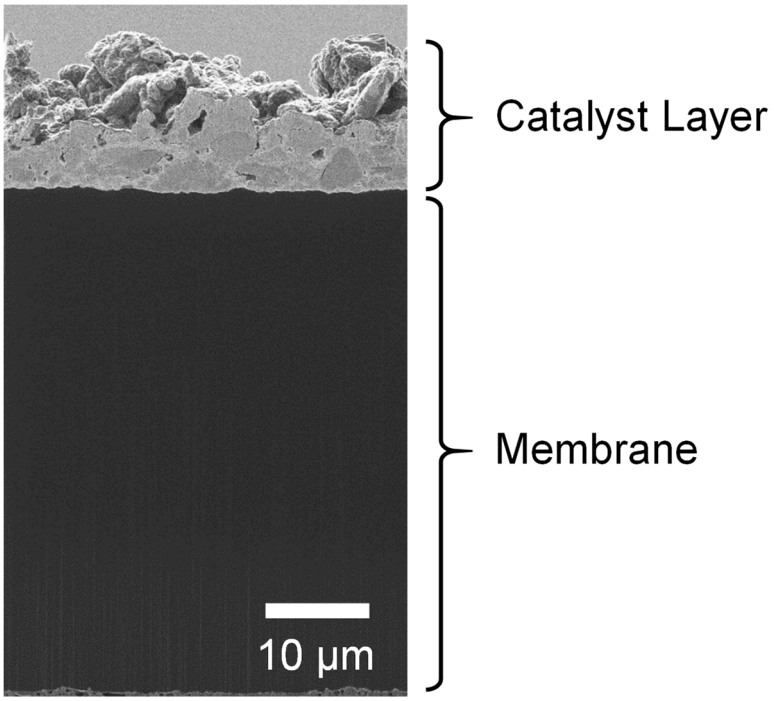


**Figure S5.** Scanning ion microscopic (SIM) image of the cross-section at the anode for the CCM with $IrO_x$/Sb-$SnO_2$ catalyst. The average thickness and the standard deviation of the catalyst layer was 9.6 ± 3.1 µm.

**Appendix S1. Calculation method for the amounts of the M-$SnO_2$ supports.**

The amount of M-$SnO_2$, for $IrO_x$/Nb-$SnO_2$ as an example, was calculated as follows. The amount of Ir loading shown in Table 1 of the text was 11.3 wt%, which was quantified by ICP after dissolving the catalysts completely by the alkaline carbonate-fusion method. This value corresponds to ($Ir^0$ + $Ir^{4+}$) contained in the catalyst, and the value of $Ir^{4+}$ ($IrO_2$) percentage analyzed by XPS was 16% (atom% = wt%). Then, we have two equations for the mass of $Ir^0$ and $Ir^{4+}$;

$$m(Ir^0) + m(Ir^{4+}) = 11.3 \quad \text{(S-1)}$$

$$m(Ir^{4+})/[m(Ir^0) + m(Ir^{4+})] = 0.16 \quad \text{(S-2)}$$

The contents of $Ir^0$ and $Ir^{4+}$ thus obtained were 9.5 wt% and 1.8 wt%, respectively. The content of $IrO_2$ [$m(IrO_2)$] can be calculated to be 2.1 wt% from the following equation:

$$m(IrO_2) = m(Ir^{4+})\times(192.22+32)/192.22 \quad \text{(S-3)}$$

Hence, the content of Nb-$SnO_2$ in the catalyst was 88.4 wt% [=100−(9.5+2.1)]. As we described in the text, we loaded a constant amount of Ir, 5 μg(Ir) $cm^{-2}$, on the Au substrate. By such a loading, the amount of Nb-$SnO_2$ loaded on the Au substrate was calculated to be 39 μg $cm^{-2}$. In the same manner, the amounts of Ta-$SnO_2$ and Sb-$SnO_2$ were estimated to be 89.3 and 88.6 wt%, respectively, as shown in Table 1, and their amounts loaded on the Au substrate were 43 and 40 μg $cm^{-2}$.

**Appendix S2. Calculation method for specific surface area of $IrO_2$ ($S_{IrO2}$) for commercial $IrO_2$ powder and $IrO_x$ nanoparticles supported on doped $SnO_2$ catalysts.**

We explain here how to calculate $S_{IrO2}$ for the $IrO_x$ particles during operation as OER catalysts. Assuming that face-centered cubic (fcc) Ir particles have an ideal cubo-octahedral shape, we calculated the number of total atoms ($N_{total}$) in the particle with the number of atomic layers ($L$) together with the number of surface atoms ($N_{surface}$), in a similar manner for the case of fcc Pt or Pt alloy particles [2,3]

$$N_{total} = (10/3)L^3 - 5L^2 + (11/3)L - 1 \quad \text{(S-4)}$$

We calculated $N_{total}$ for a spherical particle with diameter $d$,

$$d = a\,(3N_{total}/2\pi)^{1/3} \quad \text{(S-5)}$$

where $a$ is the lattice constant for Ir (fcc structure).

Next, the number of surface atoms was calculated by the following equation:

$$N_{surface} = 10L^2 - 20L + 12 \quad \text{(S-6)}$$

For the case of $IrO_x$/Nb-$SnO_2$, as an example, with $d_{Ir}$ = 2 nm, the fraction of surface atoms ($N_{surface}/N_{total}$) was calculated to be 52%. A percentage of 16% of $Ir^{4+}$ in the particle, estimated by XPS, can be rationally explained if 31% of the surface atoms (= 16/52) were oxidized to $IrO_2$ in the as-prepared catalyst. If all of the surface atoms were oxidized to $IrO_2$ with an Ir metal core during

the OER, the initial particle size of 2 nm would be nearly unchanged. Thus, the value of $S_{IrO2}$ (on an Ir metal core) was 133 $m^2\ g(Ir)^{-1}$. On the other hand, if all Ir atoms in the particle were oxidized to $IrO_2$ during the OER, the particle size could increase from 2.0 nm to 2.6 nm while maintaining a constant total amount of Ir atoms, resulting in a value of 102 $m^2\ g(Ir)^{-1}$.

In a similar manner, we calculated $S_{IrO2}$ for $IrO_x$/Ta-$SnO_2$ and $IrO_x$/Sb-$SnO_2$. The values of $S_{IrO2}$ for all catalysts are summarized in Table S1.

**Table S1.** Diameters of $IrO_x$ nanoparticles estimated by TEM ($d_{Ir}$), diameter of $IrO_2$ ($d_{IrO2}$), specific surface areas of $IrO_2$ for the $IrO_2$ shell/Ir metal core model ($S_{IrO2/Ir}$) and for the completely oxidized model ($S_{IrO2}$).

| Sample | $d_{Ir}$ (nm) | $d_{IrO2}$ (nm) | $S_{IrO2/Ir}$ [$m^2\ g(Ir)^{-1}$] | $S_{IrO2}$ [$m^2\ g(Ir)^{-1}$] |
|---|---|---|---|---|
| $IrO_x$/Nb-$SnO_2$ | 2.0 | 2.6 | 133 | 102 |
| $IrO_x$/Ta-$SnO_2$ | 2.2 | 2.8 | 121 | 95 |
| $IrO_x$/Sb-$SnO_2$ | 2.0 | 2.6 | 133 | 102 |
| commercial $IrO_2$ | – | 25 | – | 24 |

## References

1. Ohno, H.; Nohara, S.; Kakinuma, K.; Uchida, M.; Miyake, A.; Deki, S.; Uchida, H. Remarkable Mass Activities for the Oxygen Evolution Reaction at Iridium Oxide Nanocatalysts Dispersed on Tin Oxides for Polymer Electrolyte Membrane Water Electrolysis. *J. Electrochem. Soc.* **2017**, *164*, F944–F947, 10.1149/2.1101709jes.
2. Benfield, R.E. Mean Coordination Numbers and the Non-Metal Transition in Clusters. *J. Chem. Soc. Faraday Trans.* **1992**, *88*, 1107–1110, 10.1039/FT9928801107.
3. Okaya, K.; Yano, H.; Kakinuma, K.; Watanabe, M.; Uchida, H. Temperature Dependence of Oxygen Reduction Reaction Activity at Stabilized Pt Skin-PtCo Alloy/Graphitized Carbon Black Catalysts Prepared by a Modified Nanocapsule Method. *ACS Appl. Mater. Interfaces* **2012**, *4*, 6982–6991, 10.1021/am302224n.